

Analysis and prediction of windage losses and temperature fields of large flywheels

Richard Matas^{1*}, Josef Voldřich¹, Tomáš Syka¹, Jan Šlauf² and Tomáš Palek²

¹New Technologies – Research Centre, University of West Bohemia, Univerzitní 8, 301 00 Plzeň, Czech Republic

²Wikov TurboGear s.r.o., Tylova 1/57, 316 00 Plzeň, Czech Republic

Abstract. Predicting and reducing windage losses in large rotating wheels, such as those in gearboxes and flywheels, is crucial for the development of new components in the evolving energy sector. This paper is devoted to predicting windage losses in flywheels for stabilising industrial turbo machinery. It presents a large flywheel and its arrangement, along with CFD simulations and results of temperature field and windage loss predictions. A comparison of these losses with published relationships and measurements is also included, along with a case study examining the influence of specific geometric modifications and oil mist properties. The study is supported by the results of loss simulations and temperature predictions for a similar, smaller flywheel, which are again compared with measurements. The conclusion summarises the results, provides recommendations, and outlines directions for further research.

1 Introduction

The problem of windage losses caused by air resistance is becoming increasingly important in large flywheels for various purposes, electric machines, and large gearboxes currently under development. This article focuses on windage losses in large flywheels. These flywheels are typically used as energy storage devices for various purposes. In the available literature, considerable attention has been paid to losses caused by air resistance in rotating discs and gears [1], both in terms of experimental research and theoretical treatment of this problem. More recent work has dealt extensively with losses in flywheel energy storage systems for use in the energy sector, as these flywheel energy storage systems (FESS) have attracted considerable interest in the field of sustainable energy storage [6, 7, 8], where it is crucial to develop environmentally friendly methods of obtaining materials, production processes, and end-of-life waste management is vital. FESS systems are characterised by high efficiency, power density, and fast response, making them suitable for applications such as power grid stabilisation and frequency regulation, as well as the integration of renewable energy sources. Most recent work has focused on sophisticated FESS systems operating at reduced air pressure or even in near-vacuum conditions. Many of the findings from this work can be applied, but only partially, to the problem at hand, because the activities described below are devoted to the development of large flywheels for stabilising industrial turbo machinery, i.e., equipment operating under normal industrial conditions. As yet insufficiently researched issues complicate the design of these larger industrial/energy flywheels, at least in terms

of ensuring the lowest possible losses with sufficient reliability and low cost.

Most published experiments on disc windage losses were performed for Reynolds numbers an order of magnitude lower than required, or for a different key design parameter, such as wheel circumferential speed. Article [3] is an exception because, in the experiments described, the wheel was surrounded by fluid (water or oil). As a result, even though a Reynolds number of approximately 10^7 was achieved, the losses remained an order of magnitude lower than in the design we were considering.

From a design perspective, the following issues are particularly important: 1. Design geometry, including the distance between the cover and the wheel and the openings in the cover for oil drainage, etc.; 2. The properties of the oil mist inside the housing, especially between the cover and the wheel. These properties have not yet been satisfactorily determined, but they may be influenced by the cover seal and its openings, i.e., the flow inside the housing between the cover and the wheel; 3. The temperature regime of the entire flywheel installation depends on heat dissipation, the amount of oil flowing, etc. The temperature inside the flywheel housing must not exceed the temperature at which oil degradation would occur, and the temperature on the shaft also must not exceed the temperature at which the press-fit connection would come loose. On the other hand, higher temperatures result in lower losses, as will be demonstrated below.

Systematic testing to quantify the influence of the above factors on windage losses is unrealistic for large, newly designed flywheels. Not only financial and manufacturing constraints, but also time and space constraints are obstacles to such testing.

* Corresponding author: mata@ntc.zcu.cz

2 Torque scaling

Windage losses, $P = T\omega$, are the product of the frictional torque, T , and angular velocity, ω . It is helpful to distinguish between sidewall losses and losses associated with cylindrical surfaces to express T appropriately in dimensionless form. Given the small distance of the cover from the wheel compared to the size of this wheel, let us assume that these losses are independent of each other. In the case of side walls, the dimensionless torque coefficient $C_m = T / (\frac{1}{2} \rho \omega^2 a^5)$ is discussed in [3]. The relation $C_m = \frac{n}{Re^m} (\frac{s}{a})^r$, where $Re = \omega a^2 / \nu$, is proposed in this paper as the best empirical and analytical expression for the turbulent regime with separated boundary layers. Finally, for the corresponding, formula (1) is considered.

$$P_{disc} = \frac{n}{2} s^r \rho v^m a^{5-2m-r} \omega^{3-m} \quad (1)$$

We further note that measuring the latter losses is also very difficult in the case of high Taylor number

$$Ta = \sigma d^2 \left(\frac{a+b}{2}\right)^2 \omega^2 / \nu^2 \quad \text{or high Reynolds number}$$

$$Re_1 = \omega a d / \nu. \quad \text{Here } \sigma = \left(\frac{1+\eta}{2\sqrt{\eta}}\right)^4, \quad \eta = a/b.$$

Therefore, the conceptually closely related analogy between the Taylor-Couette flow and the Rayleigh-Bénard convection is applied, see [4]. Eckhardt et al. use the current J^ω of the angular velocity ω across the cylindrical gap to represent $T = 2\pi c \rho J^\omega$. The relationship between turbulent and laminar flow is given by the „Nusselt number“ $Nu_\omega = J^\omega / J_{lam}^\omega$. The dependence of Nu_ω on Ta can be obtained from the measurement results summarised in [5]. The corresponding losses can then be approximated by the formula (2).

$$P_{cylinder} = \text{const } c d^{-1+2k} \rho v^{1-2k} a^{3+2k} \omega^{2+2k} \quad (2)$$

The values of the fitted parameters in equations (1) and (2) are given in Table 1 for the assumed turbulent flow regime.

Table 1. Scaling parameters for windage losses.

n	m	r	const	k	
0.102	0.2	0.1	0.055	0.38	
m	1-2k	5-2m-r	3+2k	3-m	2+2k
0.2	0.24	2.8	3.76	2.8	2.76
ν		a			ω

It can be seen that the fitted power-law loss indices attributed to the velocity, density, and kinetic viscosity of the medium are very close for both the lateral and cylindrical walls. However, the losses of its cylindrical part increase faster with the radius of the wheel.

2.1 Dry air and oil mist

The kinematic viscosity of dry air increases sharply with increasing temperature, e.g. by 65% when the temperature rises from 50 °C to 150 °C. However, the value of ρv^m decreases, $m = 0.2$. Thus, ventilation losses (1) and (2) decrease with increasing medium temperature.

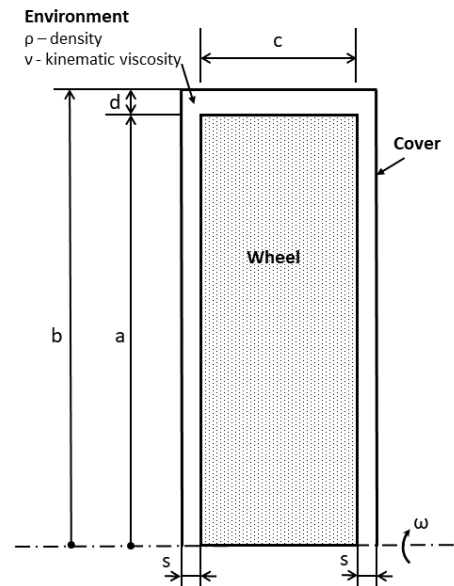


Fig. 1. Notation definition sketch.

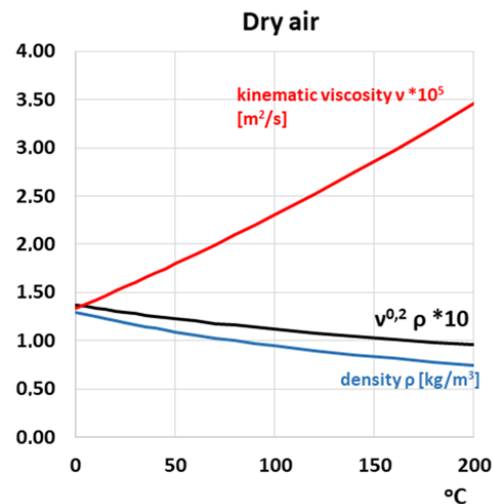


Fig. 2. Dependence of viscosity and density of dry air on temperature.

The situation is more complicated with oil mist as a medium. The relative motion between air and oil can be neglected with a very small volume of oil in this mist and under the reasonable assumption that the two phases are sufficiently well mixed by turbulence. Therefore, the dispersed oil particle size is sufficiently small [2]. The term homogeneous flow is used for such a situation, and the medium is modelled as homogeneous in the first approximation.

While the dynamic viscosity of such a medium is practically unchanged compared to dry air [2], there is a sharp increase in the average density ρ already at a small volume fraction of oil. Ventilation losses decrease with increasing oil mist temperature, as in the case of dry air, but are nominally higher. A major inconvenience that can add to these losses is that the acoustic velocity of the mist, V , decreases steeply with increasing oil volume fraction, α , approximately according to the relationship (3)(see [2])

$$\frac{1}{v^2} = \frac{1-\alpha}{kp} [\rho_{oil} \alpha + \rho_{air} (1-\alpha)], \quad (3)$$

where p is pressure and k denotes the constant pressure and volume heat capacity ratio.

3 CFD simulations

3.1 Preliminary study

A large flywheel with a diameter of almost 2 m, which was designed, manufactured, and successfully tested by Wikov TurboGear s.r.o., has gone through a development process. The design process was supported by CFD simulations with the help of knowledge from published sources. The CFD simulations were performed using the ANSYS Fluent 2024 R2 CFD system, steady turbulent flow was considered, and the turbulent model SSTk- ω . The CFD model was gradually extended to include all relevant phenomena, primarily compressibility (considering the medium as an ideal gas), the effect of external temperature T_{ext} , and external radiation. Subsequently, the effect of radiation inside the device was also considered (the S2S model supplemented by an estimate of the emissivity of the structure).

The first design proposals were considered without a wheel cover or with only partial coverage, and the first CFD models were also overly simplified. Total windage losses P_{TWL} for nominal shaft rotation speed 1800 rpm were too high than the required approx. 18 kW in these designs, see Table 2. In Table 2, it is also possible to find the maximum computed temperature of the wheel, T_{wmax} and the maximum temperature of the cover, T_{cmax} .

Table 2. Obtained values for various designs and models.

Case	P_{TWL}	T_{wmax}	T_{cmax}
	[kW]	[°C]	[°C]
1	38.4	-	-
2	33.0	-	-
3	28.7	203	181
4	26.6	187	167
5	28.6	146	123

Cases description
 1 – incompressible, without coverage, $T_{ext} = 20$ °C
 2 – incompressible, partial coverage, $T_{ext} = 20$ °C
 3 – ideal gas, without coverage, $T_{ext} = 25$ °C
 4 – ideal gas, partial coverage, $T_{ext} = 25$ °C
 5 – ideal gas, partial coverage, $T_{ext} = 25$ °C, external radiation

3.2 Flywheel development

The results above led to a redesign of the construction to cover the entire wheel. The cover design has also been developed, primarily with the aim of reducing oil inflow into the space between the cover and the wheel. Due to other requirements, oil inflow cannot be eliminated in the current design; therefore, the design must prevent oil inflow on one hand and allow oil outflow on the other. The system of holes in the cover has been adapted to this requirement.

They can see the 3D model of the facility and the flywheel manufactured at the testing facility in Figure 3.



Fig. 3. 3D model of the flywheel and finished product.

3.2.1 Study of the effect of specific parameters

A numerical study was conducted to examine several factors that affect the value of losses. The effect of internal radiation was simulated for surfaces with different emissivity ϵ (painted vs. unpainted), the effect of one larger opening in the cover vs. a design with several small holes, a smooth cover design vs. a design with "ribs," and, last but not least, the effect of the size of the gap between the cover and the disc. All values given in this chapter are for a nominal speed of 1800 rpm.

The first comparison of results was made for radiation modelling (for the cover with one larger opening at the bottom), as shown in Table 3. The obtained results show relatively small sensitivity to loss values but significant influence on temperatures. Internal radiation with an emissivity parameter of $e = 0.9$ (for painted walls) was used in further simulations.

Table 3. Obtained values for various radiation models

Case	P_{TWL}	T_{wmax}	T_{cmax}
	[kW]	[°C]	[°C]
1	15.4	185	190
2	16.0	162	162
3	16.2	154	153

Cases description
 1 – external radiation, $T_{ext} = 25$ °C
 2 – external + internal radiation, $e = 0.6$, $T_{ext} = 25$ °C
 3 – external + internal radiation, $e = 0.9$, $T_{ext} = 25$ °C

The use of only a few small holes in the cover instead of one larger hole at the bottom was also tested. The results in Table 4 show a reduction in losses for the design with small holes; however, the temperatures are higher. This design was used in further results and on the product.

Table 4. Obtained values for various openings in the cover.

Case	P_{TWL}	T_{wmax}	T_{cmax}
	[kW]	[°C]	[°C]
1	16.2	154	153
2	14.5	183	180

Cases description
 1 – ex. + int. rad., $e = 0.9$, $T_{ext} = 35$ °C, one big hole
 2 – ex. + int. rad., $e = 0.9$, $T_{ext} = 35$ °C, small holes

An investigation was also performed to add ribs to the cover and test their effect (six ribs with a thickness of 3 mm). The test was not very successful, and the performance losses with ribs are higher (0.6 kW, e.g., approximately 4%) compared to a smooth cover – see Table 5. Figure 4 shows the velocity vector field in the meridian plane and a comparison of both variants. The vortex structure on the cylindrical surface of the disc, which corresponds to the published results, is also visible.

Table 5. Obtained values for various cover structures.

Case	P_{TWL}	T_{wmax}	T_{cmax}
	[kW]	[°C]	[°C]
1	14.51	183	180
2	15.10	187	184

Cases description
 1 – ex. + int. rad., $e = 0.9$, $T_{ext} = 35$ °C, smooth cover
 2 – ex. + int. rad., $e = 0.9$, $T_{ext} = 35$ °C, cover with ribs

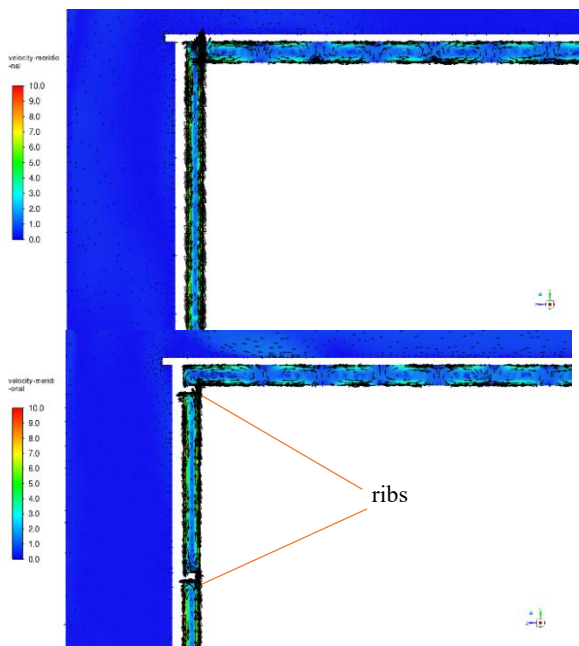


Fig. 4. Velocity vectors [m/s] in the gap between the cover and the disc for a smooth cover (top) and for a ribbed cover (bottom).

Finally, the influence of the width of the gap between the wheel and the cover was tested – see Figure 1, variables d and s . The ratio of values d and s was chosen to be fixed for the presented case, which may lead to simplified conclusions and should be expanded by a multi-parameter study. Table 6 presents the selected values of d and s , and Table 7 compares the results obtained. The separated values for sidewall losses, P_{SWL} and cylindrical losses, P_{CWL} , are presented. The results show that the value of losses initially decreases as the gap decreases, but then increases. This phenomenon is likely related to the interaction of boundary layers and warrants further investigation for various parameters. The influence of these dimensions on the maximal temperatures of components is low.

Table 6. Gap values between cover and disc.

Case	d	s
	[mm]	[mm]
1	6.0	7.5
2	9.0	11.3
3	12.0	15.0
4	18.0	22.5

Table 7. Obtained values of windage losses and maximal temperatures for various openings in the cover.

Case	P_{SWL}	P_{CWL}	P_{TWL}	T_{wmax}	T_{cmax}
	[kW]	[kW]	[kW]	[°C]	[°C]
1	7.73	6.98	14.71	186	181
2	7.62	6.51	14.13	181	177
3	7.57	6.94	14.51	183	180
4	7.745	7.43	15.18	183	182

3.2.2 Product design results and influence of the oil mist

The final design was prepared based on the results mentioned above. As already mentioned, oil mist can form in the flywheel. This is caused by its design and the attempt to remove some of the waste heat with oil.

In the first, more loss-friendly case, dry air is considered (as for all cases in the study above); in the other cases, it is oil mist, whose average density, ρ_m , corresponds to 1.25 and 1.5 times the density of dry air, ρ_a . This density corresponds approximately to 0.035 and 0.07 % oil by volume. The value of 1.5 is more in line with the medium of large gearboxes with more intensive gear spraying, but for the flywheel, a lower value of around 1.2 is likely.

Obtained values of losses and maximal temperatures for “standard” conditions (e.g. external + internal radiation, $e = 0.9$, $T_{ext} = 35$ °C) are listed in Table 8.

Table 8. Obtained values of windage losses and maximal temperatures for various medium properties.

Case	P_{SWL}	P_{CWL}	P_{TWL}	T_{wmax}	T_{cmax}
	[kW]	[kW]	[kW]	[°C]	[°C]
1	7.57	6.94	14.51	183	180
2	8.24	7.60	15.84	187	184
3	10.44	9.67	20.11	206	204

Cases description
 1 – $\rho_m/\rho_a = 1.00$ – dry air
 2 – $\rho_m/\rho_a = 1.25$ – oil mist 1
 3 – $\rho_m/\rho_a = 1.50$ – oil mist 2

As you can see, the losses increase relatively quickly with rising oil content, and this is also associated with the increase in temperature.

Figure 5 shows the final temperature field and velocity distribution between the flywheel and the cover for the basic case with $\rho_m/\rho_a = 1.00$.

4 Comparison of results

The large flywheel mentioned in the previous paragraph was tested at a nominal speed of 1800 rpm and partially at additional rpm values on the test rig in Wikov TurboGear. The temperature of all parts of the flywheel, and therefore also of the medium between the wheel and the cover, increased with the duration of the test. The end of the measurement, when the average temperature of the cover reached 180 °C, could be considered a steady state, as no further heating of the flywheel occurred.

A comparison of the above measurements and the windage losses obtained from CFD simulations, as well as values from calculations made using the method described in Chapter 2 and based on [3] and [5], is presented in Table 9. There are values for three selected "average" medium temperatures, T_m and values for simulations on given conditions. However, it was not possible to measure the oil mist properties between the cover and the wheel under severe operating conditions, so we compared the calculations for more cases.

Table 9. Comparison of calculated windage losses with measured ones

Case	T_m	ρ_m/ρ_a	P_{SWL}	P_{CWL}	P_{TWL}
	[°C]	[-]	[kW]	[kW]	[kW]
1	25	?	-	-	≈ 25 - 27
2	60	?	-	-	≈ 22 - 24
3	180	?	-	-	17 - 19
4	25	1.00	9.1	9.2	18.3
5		1.50	12.6	12.6	25.2
6	60	1.00	8.5	8.7	17.1
7		1.50	11.7	11.8	23.5
8	180	1.00	6.9	7.2	14.1
9		1.50	9.6	9.8	19.4
10	≈165	1.00	7.6	6.9	14.5
11	≈168	1.25	8.2	7.6	15.8
12	≈185	1.50	10.4	9.7	20.1

Cases description

1 to 3 – measurement

4 to 9 – computations by [3] and [5]

10 to 12 – CFD simulations

The calculations performed using the methods described in [3] and [5] are particularly attractive for fast structural design, as their input parameters can be easily entered and changed, and the results are instantaneous. It would appear from the above table that these calculations have the same informational value as the results of very demanding CFD simulations. However, they have three significant shortcomings: 1. The medium temperature needs to be entered and, therefore, calculated or estimated separately. Moreover, the temperature field depends on the magnitude of the losses; 2. CFD simulations make it possible to evaluate the influence of specific construction details (holes in the cover, seals, thermal resistances); 3. The

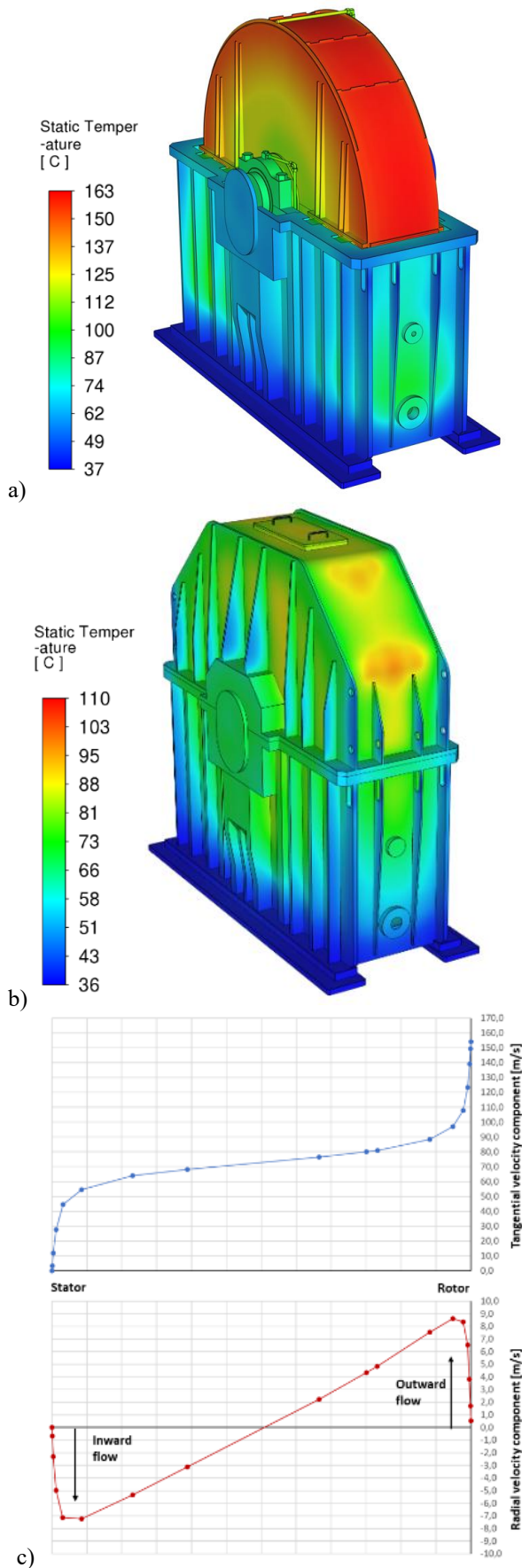


Fig. 5. Results of the flywheel CFD simulation for 1800 rpm and dry air: a) Temperature field of the cover; b) Temperature field of the housing; c) Turbulent flow velocity profiles between the housing and the wheel at a distance of 830 mm from the axis of rotation.

temperature field of the wheel, cover, and surrounding medium is not uniform. Therefore, the maximum temperature of the flywheel cannot be determined by using [3] and [5]; thus, the risk of oil degradation cannot be assessed.

The computed velocity profiles (see Fig. 5c) are consistent with the results of [3], which characterise the flow between the side walls of the cover and the wheel as turbulent with separated boundary layers for an achieved Reynolds number of approximately 10^7 .

The accuracy of the windage loss measurements in Table 9 is affected by separating the bearing losses from the total flywheel losses, which may not be straightforward [1]. We can also refine the results of the CFD calculations by determining the now missing oil mist parameters, especially in the area between the cover and the wheel.

5 Conclusions

The results of developing a large flywheel for stabilising a turbomachine were presented with the aim of accurately predicting and minimising windage losses and determining its temperature. A theoretical study was conducted, and design modifications were made based on loss predictions obtained from CFD simulations. Losses were estimated according to sources from the literature. Based on measurements, the predicted loss values obtained from analytical relationships and CFD simulations were confirmed to be sufficiently accurate. According to the simulations, maximum temperatures in individual parts of the flywheel were predicted, and they were not exceeded during the measurements.

The flywheel operates at atmospheric pressure, and unfortunately, it was not possible to use pressure reduction to minimise losses [6, 7, 8]. However, it operates at a relatively high temperature, which has a favourable effect on the magnitude of losses. Other factors influencing windage losses and the need to include them in the design were also demonstrated. The most important factor appears to be the high-quality covering of the flywheel using a cover with a suitable gap size and operation at the highest possible (yet still acceptable) temperature.

The negative effect of oil mist on losses has also been demonstrated; however, the properties have not yet been measured. The best result would be achieved by eliminating oil from the wheel and the cover area.

Another goal is to verify the methodology on another flywheel and to supplement the analytical calculation, as outlined in [3] and [5], with a fitted iterative temperature prediction model. This aims to develop a fast and sufficiently accurate tool for reliable flywheel designs, eliminating the need for 3D CFD simulations.

This study was created within the project National Centre of Competence ENGINEERING, No. TN02000018, which is co-financed from the state budget by the Technology Agency of the Czech Republic. The authors thank the company Wikov TurboGear s.r.o. for allowing the publication of measurement results obtained by their staff.

References

1. Arisawa, H., Shinoda, Y., Tanaka, M., Goi, T., Akahori, H., Yoshitomi, M., Classification and modelling of fluid dynamic loss in aeroengine transmission gears, *Journal of Engineering for Gas Turbines and Power*, **141** (6) (2019), 061012 <https://doi.org/10.1115/1.4042509>
2. Brennen, Ch.E., *Fundamentals of multiphase flow*, Cambridge University Press, 2005 <https://doi.org/10.1017/CBO9780511807169>
3. Daily, J.W., Nece, R.E., Chamber dimension effects on induced flow and frictional resistance of enclosed rotating disks, *Journal of Basic Engineering* **82**(1) (1960) 217-230 <https://doi.org/10.1115/1.3662532>
4. Eckhardt, B., Grossmann, S., Lohse, D., Torque scaling in turbulent Taylor-Couette flow between independently rotating cylinders, *Journal of Fluid Mechanics* **581** (2007) 221-250 <https://doi.org/10.1017/S0022112007005629>
5. van Gils, D.P.M., Huisman, S.G., Bruggert, G.-W., Sun, Ch., Lohse, D., Torque scaling in turbulent Taylor-Couette flow with co- and counterrotation cylinders, *Physical Review Letters* **106** (2011) <https://doi.org/10.1103/PhysRevLett.106.024502>
6. S. Venturini, S. P. Cavallaro, A. Vigliani, Windage loss characterisation for flywheel energy storage system: Model and experimental validation, *Energy*, Volume 307, 2024, <https://doi.org/10.1016/j.energy.2024.132641>
7. J. D. Nixon et al. (eds.), *Energy and Sustainable Futures: Proceedings of the 3rd ICESF, 2022*, Springer Proceedings in Energy, https://doi.org/10.1007/978-3-031-30960-1_16, 157-167
8. Y. Xie, Z. Yao, Z. Hou, X. Huang and X. Li, Experimental Investigation of Windage Loss and Steady-State Temperature in Flywheel Energy Storage Systems, 2025 7th International Conference on Power and Energy Technology (ICPET), Shanghai, China, 2025, pp. 796-801, <https://doi.org/10.1109/ICPET66029.2025.11160438>